

Hydrates and ammonium salts of 4-nitrobenzenesulfonic acid: supramolecular organization and its relation to proton conductivity

P. Yu. Barzilovich,^a K. A. Lyssenko,^{b*} M. Yu. Antipin,^b and S. M. Aldoshin^a

^aInstitute of Problems of Chemical Physics, Russian Academy of Sciences,
1 prosp. Akad. Semenova, 142432 Chernogolovka, Moscow Region, Russian Federation.
Fax: +7 (496) 515 5420. E-mail: pjetro@yandex.ru

^bA. N. Nesmeyanov Institute of Organoelement Compounds, Russian Academy of Sciences,
28 ul. Vavilova, 119991 Moscow, Russian Federation.
Fax: +7 (495) 135 5085. E-mail: kostya@xray.ineos.ac.ru

Structural features, the crystal packing, and the proton conductivity of a series of hydrates and ammonium salts of 4-nitrobenzenesulfonic acid were studied. It was shown that infinite cation associates containing the onium moiety are responsible for a substantial increase in the proton conductivity. The nature of the disorder in a series of crystals was investigated by performing X-ray diffraction studies at different temperatures. A new type of structural synthons, viz., anion-anion dimers stabilized by the $\text{SO}_3^- \cdots \text{NO}_2$ interaction, was found and characterized and the role of solvent water molecules was elucidated based on high-resolution X-ray diffraction data. The water molecules serve mainly as channels for charge transfer from the cation to the anion with retention of the electroneutrality.

Key words: sulfonic acids, proton conductivity, high-resolution X-ray diffraction studies, topological analysis, charge transfer, synthon.

The charge transfer is the fundamental value directly related to some physicochemical properties. Thus, the charge transfer is an important factor responsible for the conductivity of crystalline organic conductors.¹

One of the mechanisms of the charge transfer that actually occur most often involves the formation of hydrogen bonds, which in turn provide a versatile method for the control (design) of the desired supramolecular organization.² Thus, solid electrolytes, particularly polymeric electrolytes, considered as potential materials for various electrochemical devices (fuel cells and sensors) nearly always contain proton-generating functional groups (SO_3H , PO_3H) involved in extensive hydrogen bond networks, along which the proton transfer occurs.³ An analysis of the literature data leads to the conclusion that, in the general case, all mechanisms of the proton transfer are based on either the proton jump from a stationary acceptor to a stationary donor (Grotthuss-type mechanism)^{4,5} or the transport mechanism, where the movement of a structural group with an associated proton and the proton jump occur simultaneously.^{6,7} Water molecules, various bases, and acidic groups can act as acceptors, due to which such mechanisms are applicable to traps of any nature (so-called Bjerrum defects) and which makes it possible to vary the composition, thus controlling the ion transport. The Grotthuss-type mechanism can be consid-

ered as the most probable mechanism of the proton transport in crystals.⁸

In the present study, we investigated aromatic sulfonic acids. Due to the formation of intra- and intermolecular hydrogen bonds and high polarization of the sulfo groups in the presence of water, aromatic sulfonic acids are good model systems for the elucidation of the proton migration pathways in the crystal structures. Hydrates of aromatic sulfonic acids are of particular interest also in relation to investigations of highly hydrated forms of the proton in the crystalline state. Evidently, a system of cation-anion hydrogen bonds leads to the charge transfer from anions (for example, SO_3^-) to cations, usually such as onium ions of water (H_3O^+ , H_5O_2^+ , H_7O_3^+), ammonium, etc. The degree of the charge transfer is associated with the strength of the above-mentioned interactions.^{9,10} Taking into account that the degree of the charge transfer and the strength of hydrogen bonds can have an effect on such physicochemical characteristics of the material as the proton conductivity, these investigations are not only of interest from the fundamental point of view but are also necessary for the design of materials with high ionic conductivity.

To investigate various factors influencing the proton conductivity and elucidate the role of different types of interionic interactions (cation-anion, cation-cation, and

anion-anion) in the stabilization of a particular supramolecular organization (see, for example, the review¹⁰), we performed systematic X-ray diffraction studies, including investigations at different temperatures, to estimate the mobility of cationic and anionic moieties, and carried out high-resolution electron density distribution analysis and quantum chemical calculations for salts containing the same 4-nitrobenzenesulfonate (4-NBS) anion. Onium cations (**1**, **2**), ammonium (**3**), protonated ethylenediamine (**4**), propylenediamine (**5**), and glycine (**6**) were used as the cations. The choice of the nature of the cations was determined by the possibility of creating a convenient model for investigation of the influence of the supramolecular organization on the proton conductivity. In addition, this anion is of interest because both dihydrate and tetrahydrate of 4-nitrobenzenesulfonic acid can be obtained by varying the starting concentration of the acid in water.¹¹

Results and Discussion

In all the compounds under study, the main geometric parameters of the 4-NBS anion are almost identical (Fig. 1). In the crystal structures, the sulfo groups exist in the deprotonate form, and the S—O distances vary in the range of 1.448(1)—1.477(1) Å, a slight elongation of the S—O bond being observed for the oxygen atoms involved in the largest number of hydrogen bonds. In the whole series of the compounds, the S(1)—C(1) and C(4)—N(1) bond lengths remain virtually unchanged (1.774(1)—1.780(1) and 1.468(2)—1.470(1) Å, respectively). In all compounds, the nitro group is coplanar, within experimental error, with the plane of the benzene ring. On the contrary, the rotation of the SO₃[−] groups with respect to the aromatic ring is determined by a hydrogen bonding system and, as will be shown below, may vary depending on the temperature of the X-ray diffraction experiment.

First, let us consider the onium salts of 4-NBS. As mentioned above, dihydrate (**1**) and tetrahydrate (**2**) containing the Zundel ion H₅O₂⁺ and the Eigen-type ion H₇O₃⁺ as the cations (Figs 2 and 3, respectively) were

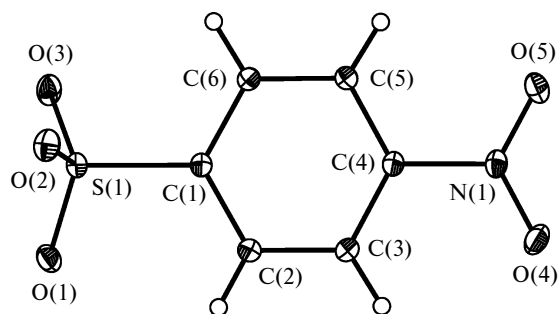


Fig. 1. General view of the 4-nitrobenzenesulfonate anion with displacement ellipsoids ($p = 50\%$).

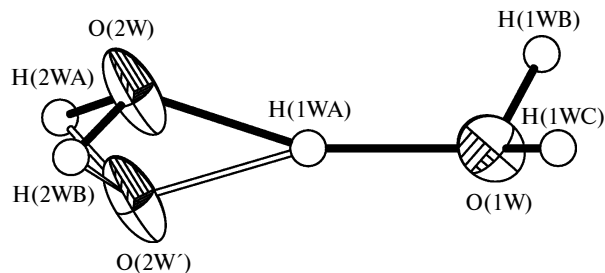


Fig. 2. General view of the Zundel ion in dihydrate **1** with displacement ellipsoids ($p = 50\%$).

isolated and characterized by varying the initial concentration of 4-NBS in water. The conclusion about the type of the cation associate was drawn based on the positions of the localized protons and the O...O distances between the proton acceptor and donor. As it can be seen, one of the oxygen atoms, O(2W), is disordered in both cations.

In the crystal structure of **1**, the O(1W)...O(2W) and O(1W)...O(2W') distances in the H₅O₂⁺ cation are 2.436(2) and 2.413(2) Å, respectively, the H(1WA) proton being almost symmetrically located between the oxygen atoms (the H(1WA)—O(1W), H(1WA)—O(2W), and H(1WA)—O(2W') distances are ~1.23 Å). This geometry of the cation and the relatively large isotropic displacement parameter of the H(1WA) atom (0.08(2) Å² compared with 0.037(9)—0.07(1) Å² for the other hydrogen atoms of the H₅O₂⁺ cation) suggest that this cation is disordered over two positions, which is quite typical of strong hydrogen bonds (see Ref. 12 and references herein). Based on the aforesaid, it cannot be ruled out that the positions of the O(2W) and O(2W') atoms with occupancies of 0.621(4) and 0.379(4), respectively, located in difference Fourier maps correspond to the oxonium and "water" components of the cation. This cation forms strong hydrogen bonds with the SO₃[−] groups of the anions (O...O, 2.650(2)—2.757(2) Å), the hydrogen bonds formed by the O(1W) atom being somewhat shorter, which is more typical of the onium ion.

In the crystal structure of tetrahydrate **2**, as opposed to dihydrate **1**, there are infinite cationic chains containing H₇O₃⁺ ions, as follows from the much shorter O(1W)...O(4W), O(1W)...O(2W), and O(1W)...O(2W')

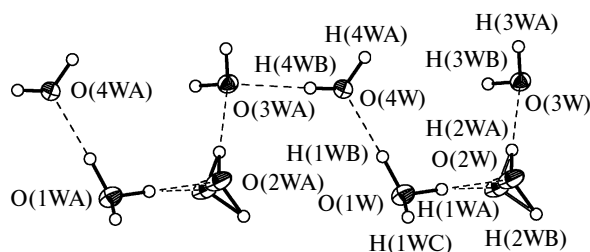


Fig. 3. General view of the H₇O₃⁺ ion in tetrahydrate **2** with displacement ellipsoids ($p = 50\%$).

distances (2.499(1), 2.505(1), and 2.492(2) Å, respectively; in **1**, the O(2W)...O(3W) and O(4W)...O(3WA) distances are 2.770(1) and 2.758(1) Å) (see Fig. 3). As opposed to the dihydrate, strong hydrogen bonds in tetrahydrate **2** are characterized by pronounced asymmetry, resulting in that the H(1WA) and H(1WB) protons form stronger bonds with the O(1W) atom (0.85–0.92 Å) than with the O(4W), O(2W), and (O(2W') atoms (1.58–1.60 Å).

The other hydrogen atoms of the cationic chains in **2** are involved in the formation of cationic hydrogen bonds (O...O, 2.657(1)–3.148(1) Å) typical of sulfonic acids. As in the case of **1**, the shortest distances between the proton donor and acceptor are observed for the onium oxygen atom O(1W), whereas the longest distances (2.816(1)–3.148(1) Å) are observed for the formally solvent water molecule O(4W).

In the crystal structure of **2**, the occupancies of two components of the O(2W) atom are substantially different and are 0.884(3) and 0.116(3) for O(2W) and O(2W'), respectively, at 100 K (see Fig. 3). The X-ray diffraction studies of **2** performed at higher temperatures showed that the disorder has the dynamic character. Thus, at 173 and 250 K the occupancy of the O(2W') position increases to 0.199(7) and 0.275(8), respectively. It should be noted that, as in the crystal structure of **1**, the isotropic temperature factor of the H(1WA) proton (0.067(5) Å²) involved in the hydrogen bonding with the disordered oxygen atom is larger than that for the H(1WB) proton (0.046(3) Å²). A similar relation is retained as the temperature increases to 250 K (0.101(10) and 0.087(8) Å²). It should be noted that the larger temperature factor cannot be attributed to the stronger hydrogen bond and, consequently, to an increase in the vibrational amplitude because the O(1W)...O(4W) and O(1W)...O(2W) distances are slightly shorter regardless of the temperature. It is interesting that, except for variations in the occupancies of two O(2W) positions, the other molecules/ions in **2** remain ordered.

This disorder, which has been observed earlier in other sulfonic acids,¹³ may be attributed both to the inversion of the oxygen atom¹⁴ and the above-mentioned superposition of the "water" and "onium" components of the cation. Earlier we have shown that the lone pair of the onium ion is actually not revealed by topological analysis of the electron density distribution function, as well as by the analysis of the electron pair localization function and is "inert" with respect to the formation of specific interactions in the crystals.¹⁵ However, taking into account very low barrier of the inversion (about 1 kcal mol⁻¹),¹⁴ it would be expected that the occupancies of two oxygen positions are equal, but this was not observed experimentally. Hence, the above-described disorder in the crystals of **1** and **2** is most likely attributed to the proton transfer, and the nonequivalence of the positions is, in turn, due to the difference in the environment of the atoms in the crystals resulting in the different strength of the hydrogen bonds

for two tautomers.¹⁶ It should be emphasized that the localization of the position of the disordered O(2W) atom in salt **2** at 100 K became possible due to the high resolution of the X-ray diffraction data ($2\theta_{\text{max}} = 100^\circ$), whereas it is impossible to localize this weakly occupied position of the oxygen atom (to be more precise, to suggest the presence of this position) in the routine experiment. Hence, it cannot be ruled out that the observed disorder has a more general character and may be observed in the formally "ordered" (according to the literature data¹⁷) crystal structures, resulting in systematic errors in the determination of the O...O and O—H distances characterizing the strength of the hydrogen bonding.

Apparently, the presence of an infinite hydrogen-bonded network formed by water molecules and the onium ion in tetrahydrate **2** as opposed to the discrete system of hydrogen bonds (SO₃⁻...H₅O₂⁺...SO₃⁻...H₅O₂⁺) in dihydrate **1** (Fig. 4) leads to an increase in the specific proton conductivity by more than 1.5 orders of magnitude (from 10⁻⁶ to 10⁻⁴ S cm⁻¹ at room temperature). This fact is in good agreement with the assumed Grotthuss-type mechanism of the proton transfer in onium salts **1** and **2**. Taking into account that the disorder of the oxygen atom may be in part considered as a structure defect, it can be hypothesized that its presence is also favorable for an increase in the specific proton conductivity.

It should be noted that, in spite of the dramatically different character of the cation associates, the arrangement of the anions in salt **1** is almost identical to that in **2**. As it can be seen from the projections of the crystal packing (see Fig. 4), the anions are arranged in head-to-tail stacks in both structures. Based on the interplanar distances, it may be concluded that the anionic columns in **1** and **2** are involved both in stacking interactions between the aromatic systems and in quite unusual O₂S—O⁻...O₂N-type interactions. Thus, pairs, which are linked together predominantly by short O...N interactions (2.991(1) Å) characterized by the distinct directionality (the angle between the O(1)...N(1A) line and the plane of the nitro group is 86.5°), as well as dimers stabilized by stacking interactions (the shortest C(3)...C(1A) distance is 3.480(1) Å), are observed in the anionic columns in the crystal structure of **2** (Fig. 5). In the crystal structure of **1**, there are apparently no stacking interactions in the columns (the C...C distances (3.932(2) Å) are larger than 3.55 Å), and the O...N anion—anion interactions are somewhat shorter (2.839(2) Å). These anion—anion interactions are similar in nature to the interactions between nitrate anions¹⁰ and, apparently, correspond to the charge transfer from the lone pair of the oxygen atom to the antibonding orbital of the nitrogen atom of the nitro group.

Within the associates stabilized by both stacking interactions and strong intermolecular interactions, the charge transfer is always observed. It should be noted that the conductivity determined by the presence of stacks of aro-

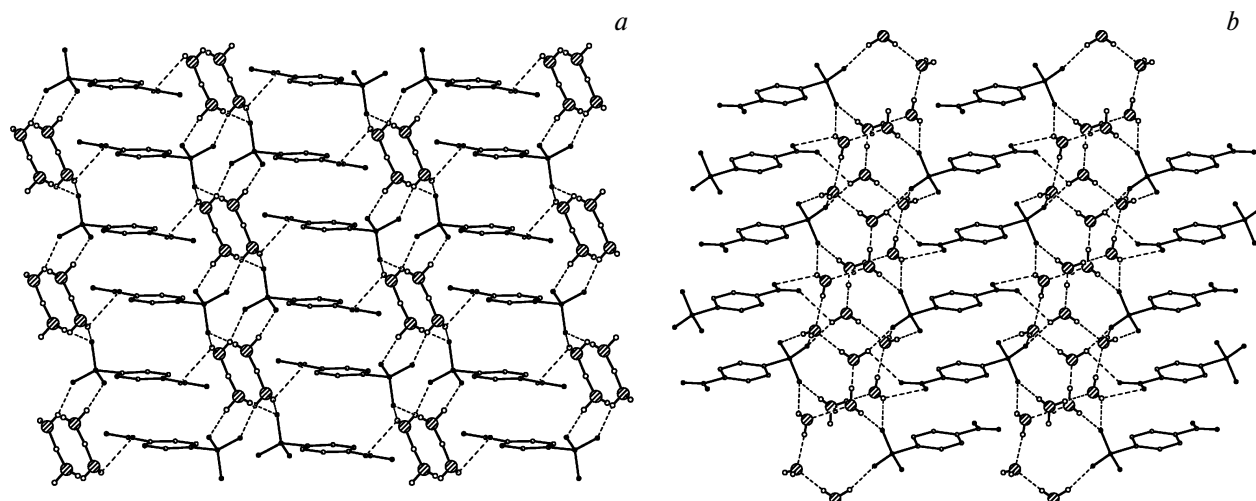


Fig. 4. Fragments of the crystal packing of di- (a) and tetrahydrate (b) of 4-NBS. The oxygen atoms of the cation associates are shown as dashed circles.

matic π systems is several orders of magnitude smaller than the measured proton conductivity. For example, the conductivity of the complexes based on trinitrobenzene with polycyclic aromatic compounds is 10^{-14} – 10^{-20} S cm $^{-1}$.¹⁸ It should be emphasized that such associates are of primary importance in the conductivity of DNA.¹⁹

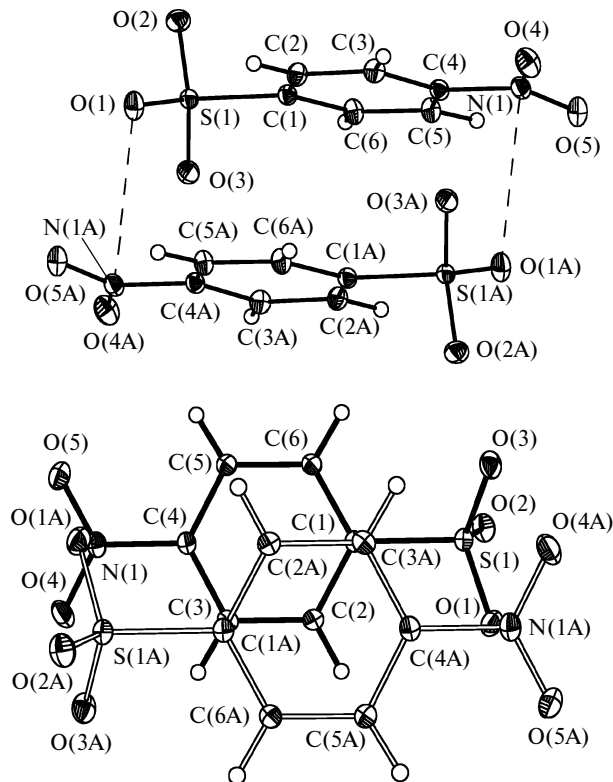


Fig. 5. Dimers in the anionic columns in tetrahydrate **2** formed through $\text{SO}_3\cdots\text{O}_2\text{N}$ contacts and stacking interactions.

The unusual fact is that anionic columns are present not only in the above-considered hydrates **1** and **2** but also in all other salts of 4-NBS under study regardless of the nature of the cation. For example, in the crystals of ammonium salt **3**, in which the SO_3^- groups are disordered over two positions with occupancies of 0.336(2) and 0.664(2) at 100 K, both positions are involved in the above-mentioned interactions ($\text{O}\cdots\text{N}$ and $\text{O}\cdots\text{O}$ distances are ~ 2.88 and 2.77 Å, respectively), resulting in the formation of dimers. The dimers are linked to each other by stacking interactions, which are substantially weakened due to a large shift of the anions and, consequently, a small overlap of the π systems. In the crystal structure of protonated ethylenediamine monohydrate (**4**), in which discrete cation associates are also present (Fig. 6, a), the character of interactions between the anions in the columns is identical to that observed in dihydrate **2**: the alternating dimers of the anions linked together by stacking interactions with the shortest C...C distances of $3.456(1)$ Å and dimers linked to each other by $\text{SO}_3^-\cdots\text{NO}_2$ interactions with the $\text{O}\cdots\text{N}$ and $\text{O}\cdots\text{O}$ distances of $2.783(1)$ and $3.108(1)$ Å, respectively.

A somewhat different character of the supramolecular organization of the anions is observed in the crystal structure of protonated propylenediamine monohydrate (**5**), in which, as opposed to **3** and **4**, there are infinite cation associates (Fig. 6, b). In the crystal structure of salt **5**, there are two symmetrically independent anions (*A* and *B*). These anions form $A\cdots B\cdots B\cdots A$ tetramers, in which the $A\cdots B$ anions are arranged perpendicular to each other, whereas the $B\cdots B$ anions are parallel to each other (Fig. 7). The directional $\text{SO}_3^-\cdots\text{O}_2\text{N}$ interactions with the $\text{O}\cdots\text{N}$ distances of $2.816(1)$ and $2.956(1)$ Å belong to the main type of interactions stabilizing the tetramers.

However, in the crystal structure of hydrate of the salt of 4-NBS with glycine (**6**), which contains even larger

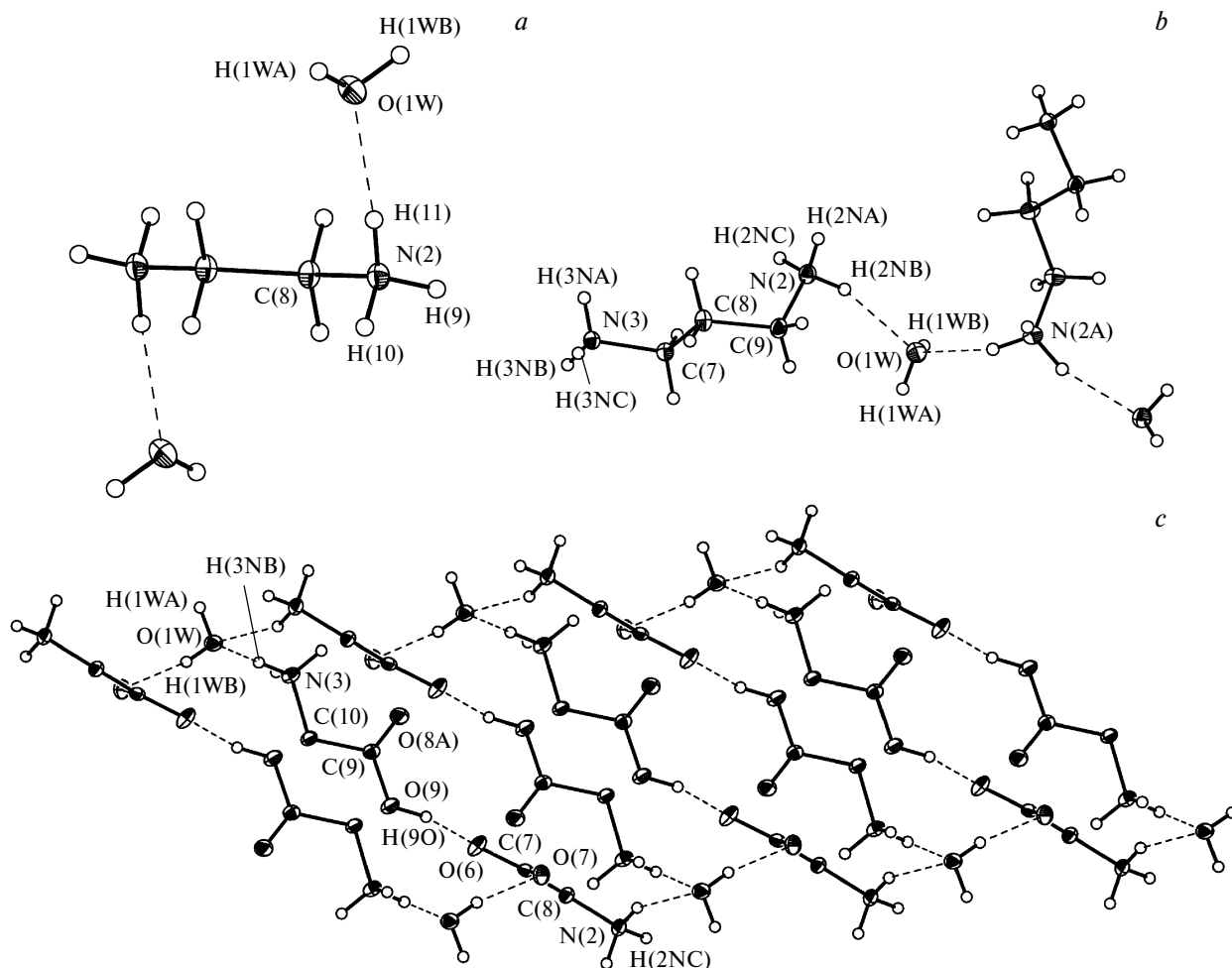


Fig. 6. Cation associates in the crystal structures of the salts of 4-NBS: monohydrates of protonated ethylenediamine **4** (a), propylenediamine **5** (b), and glycine **6** (c). The N(2)...O(1W) distances in salts **4** and **5** are 2.762(1) and 2.816(1) Å, respectively. The O(9)...O(6), N(3)...O(1W), O(7)...O(1W), and N(2)...O(1W) distances in salt **6** are 2.541(2), 2.738(2), 2.742(2), and 2.870(2) Å, respectively.

cation associates, *viz.*, the chains consisting of the Zundel-type cations $[\text{NH}_3\text{—CH}_2\text{—CO}_2\text{...H—OC(O)CH}_2\text{NH}_3]^+$ linked by water molecules (Fig. 6, c), there are also anion-anion associates identical to those found in the crystals of **1**, **4**, and **5**; the distances between the $\text{O}_2\text{S—O}^-$ and NO_2 groups are 2.734(2) Å.

An analysis of the Cambridge Structural Database (CSD) of related compounds (*i.e.*, compounds containing anions, in which sulfo and nitro groups are present in positions 1 and 4 of the aromatic ring) showed that the above-mentioned anion-anion associates are present in 17 of 47 structures (including those described in the present study), *i.e.*, in 36% cases. In most cases, where these anion-anion associates are not present in the crystal structures, aromatic or heterocyclic systems serve as cations, which are involved in the formation of cation-anion dimers through stacking interactions. Therefore, it can be concluded that the associates under considerations, in spite of

the fact that they should be unfavorable due to the anion-anion character, can be considered as supramolecular synthons²⁰ and, consequently, should be taken into account in the design of proton conductors.

In spite of the difference in the supramolecular organization of the cations in the ammonium salts (the presence of infinite associates in **5** and discrete associates in **4**), these salts have almost the same conductivity at room temperature (10^{-9} – 10^{-10} S cm⁻¹). However, in both cases an increase in the temperature to 160–180 °C led to an increase in the specific conductivity to 10^{-6} S cm⁻¹. It should be noted that, according to the thermogravimetric data for these samples, the water loss is observed at 120–130 °C. Hence, the measured conductivity in fact corresponds to the anhydrous forms of salts **4** and **5**. Most probably, the librational motion of the SO_3^- groups in the crystals of **4** and **5** will be substantially larger at 160–180 °C as a result of the water loss. In these cases, the conductiv-

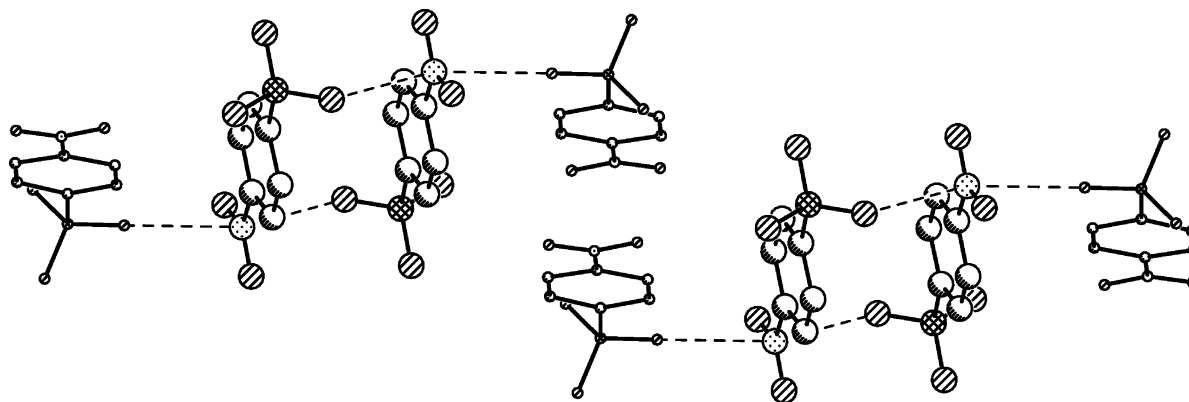


Fig. 7. Fragment of the crystal packing of protonated propylenediamine 4-NBS monohydrate (**5**). The atoms of the independent anion *B* are shown as larger circles.

ity will be provided by the proton jump from the cation to the SO_3^- group of the anion followed by the proton transfer to another amine molecule, which will allow the proton to migrate in the bulk of the crystal.²¹ Therefore, it may be supposed that the transport mechanism of the proton transfer in salts **4** and **5** becomes dominant with increasing temperature.

To a certain degree, this mechanism of the proton transfer is consistent with the results of the X-ray diffraction studies of **4** and **5** at room temperature. According to these data, even in the presence of water molecules in both salts, an increase in the temperature by 120 °C leads to the disorder of the SO_3^- groups in ratios of 0.50(2), 0.50(2) and 0.868(11), 0.132(11) in two independent anions of compound **5** and in a ratio of 0.868(5), 0.132(5) in compound **4**. The differences in the ratio of two positions of the SO_3 groups in **5** are in good agreement with the strength of the above-described $\text{SO}_3^- \cdots \text{NO}_2$ interactions. Taking into account that the further rise of the temperature and the water loss will lead to an increase in the mobility of the SO_3^- groups, the proposed scheme of the dominant transport mechanism of the proton transfer is highly probable.

To study in detail the nature of the above-described anion-anion associates and to analyze the role of solvent water molecules in the charge transfer between the anion and the cation, we performed the topological analysis of the total electron density distribution functions for salts **2**, **4**, and **5**, which were derived from the high-resolution X-ray diffraction data, within Bader's theory of Atoms in Molecules.²² The energy of interactions was estimated based on the semiquantitative Espinosa—Lecomte correlation,²³ which was developed and successfully used for the description of a wide range of weak, including dispersion, interactions in the crystals.²⁴ The advantages of this approach in studying the nature of chemical bonding and estimating the strength of cation-anion interactions have been considered in our earlier study.¹⁰ Taking into account the facts that the cationic layer in the crystals of

dihydrate **2** is disordered and that the electron density distribution, at least in the region of the H_7O_3^+ cation, may have systematic errors, we performed quantum chemical calculations of the neutral cluster containing a fragment of the crystal packing of onium salt **2** consisting of the anion-anion dimer surrounded by two cation associates, which include six water molecules and the onium cation (Fig. 8). For this cluster, we performed the full geometry optimization with the use of the B97D dispersion-corrected functional²⁵ and the 6-311+G** basis set.

First, let us consider the results of quantum chemical calculations. In spite of the fact that the optimization was performed without symmetry constraints, the cluster under consideration has the symmetry C_i . It is interesting that the level of theory used in the calculations allowed us to reproduce the geometric features observed in the crystal with high accuracy, which is of obvious methodological interest. In particular, the O(1W) ... O(2W) distance in the isolated cluster (2.512 Å) is only slightly larger than that (2.499(1) Å) in the crystal of **2**. It should be noted that in the isolated cluster, as opposed to the crystal, three hydrogen atoms are localized at the O(2W) atom (all O—H distances are at most 1.05 Å) rather than at the O(1W) atom. Based on the O ... O distances in the cluster, it may be supposed that it contains the H_7O_3^+ cation rather than $\text{H}_{11}\text{O}_5^+$. Actually, the O(3W) ... O(2W), O(2W) ... O(1W), O(2W) ... O(5W), and O(5W) ... O(7W) distances (2.515–2.654 Å; the largest distance is observed between the O(5W) and O(7W) atoms) are substantially shorter than the corresponding distances between the O(4W) atom and the O(1W), O(3W), and O(6W) atoms (2.809–2.821 Å).

An analysis of the charges determined by the integration of the electron density distribution function over atomic basins showed that it is difficult to precisely assign the charged cation to a particular type because the net charges of all oxygen atoms with those of the attached hydrogen atoms (except for the O(2W) atom) gave zero.

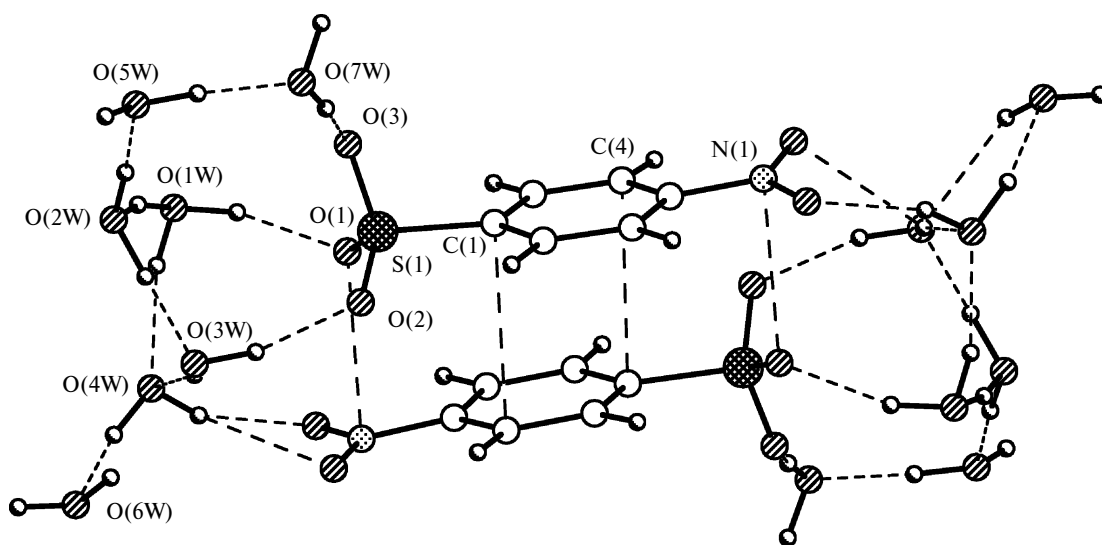


Fig. 8. General view of the model cluster containing a fragment of the crystal packing of onium derivative **2** based on the results of B97D/6-311+G** calculations.

For example, the charge of $\text{H}_3\text{O}(2\text{W})^+$ is 0.67 e, whereas the charges of the other water molecules vary from 0.005 to 0.05 e. The character of hydrogen bonds in the cation associates can be considered as the more reliable criterion for the determination of the type of the cation. Actually, negative values of the local electron energy density $h_e(\mathbf{r})$ (-0.06 – 0.09 a.u.) with positive values of the Laplacian of the electron density $\nabla^2\rho(\mathbf{r})$ at the corresponding critical points (3, -1) are observed only for the $\text{O}(1\text{W})\cdots\text{H}\cdots\text{O}(2\text{W})$, $\text{O}(2\text{W})\cdots\text{H}\cdots\text{O}(3\text{W})$, and $\text{O}(2\text{W})\cdots\text{H}\cdots\text{O}(5\text{W})$ hydrogen bonds. Therefore, these hydrogen bonds correspond to the intermediate type of interatomic interactions, whereas the other hydrogen bonds in the cationic cluster are characterized by either positive values of $h_e(\mathbf{r})$ or near-zero values (-0.001 a.u.), and, correspondingly, they belong to closed-shell interactions. The difference in the type of interactions reflects the different degrees of covalency of the hydrogen bonds and is in good agreement with the higher energy (17 – 28 kcal mol $^{-1}$) compared with the other hydrogen bonds formed by water molecules (~ 8.5 kcal mol $^{-1}$), as well as with cation-anion interactions (6 – 8.2 kcal mol $^{-1}$). Consequently, the topological analysis of $\rho(\mathbf{r})$ in the cation associate leads to the conclusion that the H_7O_3^+ cation is present both in the crystals and in the isolated cluster in spite of variations in the strength of interactions. In turn, the analysis of the short interactions between the anions showed that the anion-anion associates selected based on the geometric criteria are actually stabilized by both stacking interactions ($\text{C}\cdots\text{C}$, 3.380 Å) and interactions between the SO_3^- and NO_2 groups ($\text{O}\cdots\text{N}$, 3.015 Å). These interactions belong to the closed-shell type and, in spite of the relatively low energy (0.76 and 1.76 kcal mol $^{-1}$, respectively), can stabilize dimers and infinite columns in the crystals. This is actually observed in com-

pounds **1**–**5**. The topological parameters of the anion-anion interactions in the crystals of **2**, **4**, and **5** determined by quantum chemical calculations are in good agreement with the results of high-resolution X-ray diffraction studies.

For an additional illustration of how precise is the experimental electron density distribution function, particularly for the crystal of **2** characterized by the disorder of the cation, we analyzed the deformation electron density distribution. As it can be seen from the deformation electron density maps, the observed distribution is similar to the expected one both for hydrogen bonds and covalent interactions (Fig. 9).

According to the results of the topological analysis, the $\text{SO}_3^-\cdots\text{NO}_2$ interactions are bonding in all three crystal structures, as evidenced by the presence of the critical point (3, -1) and the bond path that links the corresponding oxygen and nitrogen atoms. The topological parameters of these interactions vary in a narrow range ($\rho(\mathbf{r}) = 0.05$ – 0.08 e Å $^{-3}$; $\nabla^2\rho(\mathbf{r}) = 0.83$ – 1.11 e Å $^{-5}$) determined primarily by the $\text{O}\cdots\text{N}$ distances. Thus, the strongest interaction is observed in the crystal structure of **4**; the $\text{O}\cdots\text{N}$ distance is $2.783(1)$ Å, and the energy of this interaction is 2.4 kcal mol $^{-1}$. The weakest interaction is observed in the crystal of **2** ($\text{O}\cdots\text{N}$, $2.991(1)$ Å) with the energy of 1.35 kcal mol $^{-1}$. It should be noted that the observed difference in the strength of the interactions in **5** (1.4 and 2.1 kcal mol $^{-1}$) for two independent anions is in good agreement with the difference in the occupancy of two positions of the disordered SO_3^- group at room temperature. As it can be seen from the deformation electron density map in the vicinity of the $\text{SO}_3^-\cdots\text{NO}_2\cdots\text{SO}_3$ interaction in salt **5** (Fig. 10), these interactions can be described as the charge transfer from the lone pair of the

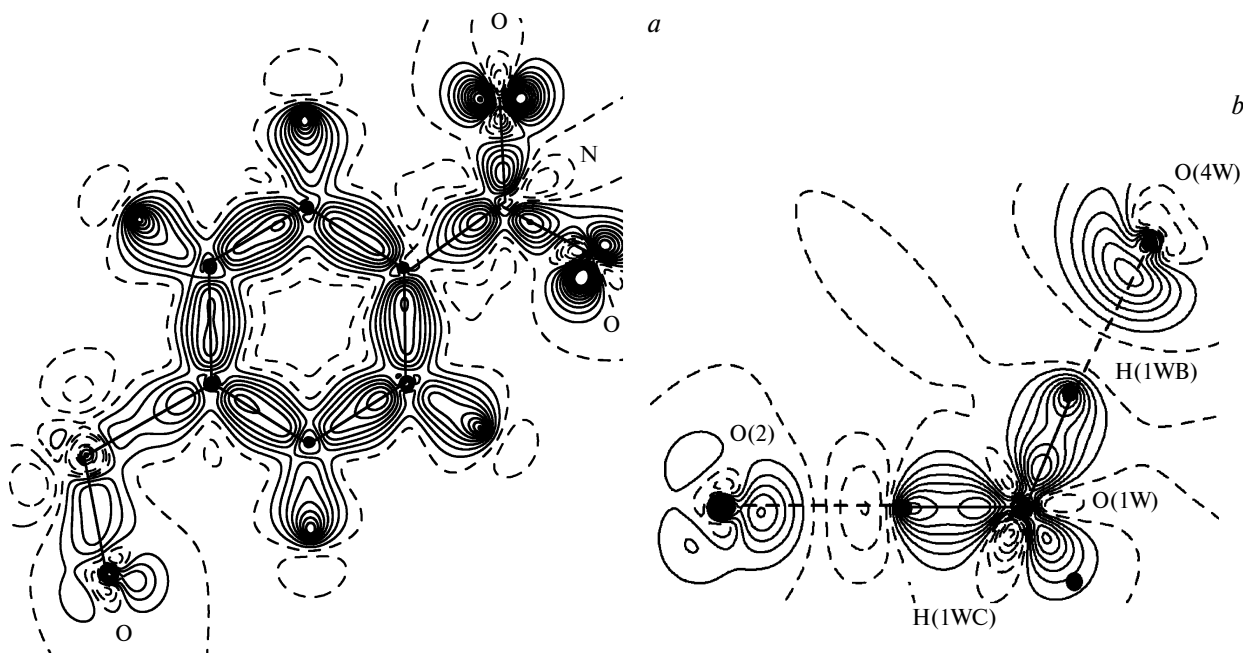


Fig. 9. Deformation electron density maps for the anion (*a*) and in the vicinity of $\text{SO}_3^- \cdots \text{H}_3\text{O}^+ \cdots \text{H}_2\text{O}$ hydrogen bonds in the crystal of **2** (*b*) contoured at $0.05 \text{ e} \cdot \text{\AA}^{-3}$ intervals; the negative values are indicated by dashed lines.

oxygen atom to the antibonding orbital of the nitrogen atom of the NO_2 group.

In addition to the $\text{SO}_3 \cdots \text{NO}_2$ interactions between the anions, there are stacking interactions involving the aromatic rings. However, the energy of the latter, as in the case of the isolated model cluster (see above), is substantially lower ($0.65 \text{ kcal mol}^{-1}$).

Therefore, a combined experimental and theoretical study of the electron density distribution and the analysis of the CSD provide convincing evidence that the unusual stabilization of anion-anion associates in the crystals of 4-nitrobenzenesulfonate salts is attributed to specific $\text{SO}_3^- \cdots \text{NO}_2$ interactions.

Since hydrogen bonds ensure the main channel for charge transfer in these salts, it was also interesting to analyze whether the electroneutrality of the water molecules involved in different (cation-cation and cation-anion) hydrogen bonds, which was determined by quantum chemical calculations of the model cluster, will be observed in the crystals, in which the cation-anion interac-

tions are much stronger and, as a result, the charge transfer from the anion to the cation is more pronounced.

The analysis of the charges determined by the integration of $\rho(\mathbf{r})$ over atomic basins showed that the total charge in the crystals of **4** and **5** is equal to zero ($0 \pm 0.01 \text{ e}$) regardless of the character of hydrogen bonds. In both crystals, a substantial charge redistribution from 0.24 to 0.55 e is observed. Its value is governed by the number and strength of cation-anion hydrogen bonds. It should be noted that in the salts of sulfonic acids studied earlier,^{9,13a} the charge transfer correlates, on the whole, with the energy of hydrogen bonds. Therefore, solvent water molecules act predominantly as channels for charge transfer from cations to anions both in the ammonium and onium salts.

We studied a series of 4-nitrobenzenesulfonic acid derivatives with different cations. It was shown that the supramolecular organization of ionic associates, as well as a slight disorder of the corresponding structural fragments, has an effect on the integrated value of the specific ionic conductivity. The analysis of the electron density distribution revealed a new structural synthon, which can be used for the design of proton conductors.

The possibility to construct the correlations between the charge transfer and the energy of cation-anion interactions in compounds **2**, **4**, and **5** and in isolated model clusters will be investigated and discussed in detail elsewhere.

Experimental

Hydrate **1** was synthesized by the hydrolysis of commercial 4-nitrobenzenesulfonic chloride (Fluka) with a 1 : 1 diox-

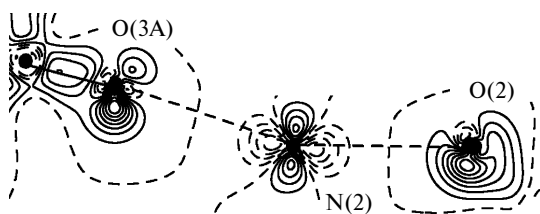


Fig. 10. Deformation electron density map in the vicinity of the $\text{SO}_3 \cdots \text{NO}_2 \cdots \text{SO}_3$ interaction in the crystal of **5**.

ane—water mixture for 3 h. The evaporation of the reaction mixture gave yellowish prismatic crystals. Hydrate **2** was isolated based on the phase diagram.¹¹ Salts **3**–**6** were prepared by slow evaporation of aqueous solutions of an equimolar mixture of the acid and the corresponding amio compounds.

The proton conductivity was measured on a Z-2000 impedance meter (Elins Ltd) (operating frequencies were in the range from 2 MHz—1 Hz) using C/solid electrolyte/C symmetrical cells. The amplitude of the external alternating signal was 50—150 mV depending on the impedance of the sample without direct-current polarization. The frequency dependence of the resistance was analyzed by the graphical analytical method.²⁶ It should be noted that a substantial contribution of the electrode impedance to the cell resistance was observed in none of the cases. This conclusion was supported by the fact that the impedance was independent of the nature of the electrodes (carbon paper, platinum). The samples placed in the cells were prepared as pressed (the pressing pressure was 5 atm) pellets 0.5—1.1 mm thick and 5 mm in diameter.

The thermal stability of the samples was determined by differential scanning calorimetry (DSC) followed by mass spectrometric analysis of the decomposition products on Netzsch STA 409 PC LUX and QMS 403 C Aeolos instruments. The TGA spectra were recorded in the temperature range of 298—873 K; the heating rate was 5—10 K min^{−1}.

An analysis of the thermogravimetric behavior of 4-nitrobenzenesulfonic acid dihydrate and tetrahydrate showed that the dehydration started in the ranges of 95—103 °C and 75—80 °C, respectively. This behavior can be attributed to the different degrees of interactions between the sulfo group and water cat-

ions. The onset of the decomposition of the anions occurred at 190 °C and was accompanied by elimination of sulfur oxides and thermal decomposition products of the nitrobenzene moiety.

X-ray diffraction study was performed on a Bruker SMART Apex II CDD diffractometer ($\lambda(\text{Mo-K}\alpha) = 0.71072 \text{ \AA}$). The structures of **1**–**6** were solved by direct methods and refined by the full-matrix least-squares method with anisotropic displacement parameters based on F^2_{hkl} . The hydrogen atoms were located in difference Fourier maps and refined isotropically. Main crystallographic data and the structure refinement statistics for all structures are given in Tables 1 and 2. All calculations were carried out with the use of the SHELXTL-97 program package.²⁷

The multipole refinement of the structures of **2**, **4**, and **3** was carried out within the Hansen—Coppens model²¹ with the use of the XD program package.²⁸ In the multipole refinement, the coordinates, the anisotropic displacement parameters, and the multipole parameters up to the octupole level ($l = 3$) for all nonhydrogen atoms were refined against F_{hkl} . The positions of the hydrogen atoms and their isotropic displacement parameters were kept fixed. Before the refinement, all C—H distances were normalized to the ideal distance (1.08 Å), and the O—H and N—H distances were taken from the neutron diffraction data for similar structures and the results of quantum chemical calculations for the model cluster. For the more correct description of hydrogen bonds, the electron density for the hydrogen atoms was described by dipoles and hexadecapoles taking into account the cylindrical symmetry. The correctness of the anisotropic atomic displacement parameters was estimated using the Hirshfeld test, which was no larger than $6 \cdot 10^{-4} \text{ \AA}^2$. The results of the

Table 1. Main crystallographic data and the structure refinement statistics for onium derivatives **1** and **2**

Parameter	1		2	
Molecular formula	C ₆ H ₉ NO ₇ S		C ₆ H ₁₃ NO ₉ S	
Molecular weight	239.20		275.23	
<i>T</i> /K	100	100	173	275
Crystal system	Monoclinic		Triclinic	
Space group	<i>P</i> 2 ₁ / <i>n</i>		<i>P</i> -1	
<i>Z</i>	4		2	
<i>a</i> /Å	7.4634(7)	6.4206(1)	6.4353(5)	6.4556(8)
<i>b</i> /Å	7.2360(6)	7.5945(1)	7.6048(6)	7.6466(9)
<i>c</i> /Å	18.2806(16)	11.9438(2)	11.9592(10)	12.0175(14)
α /deg	90.00	97.1823(8)	97.2157(14)	97.226(2)
β /deg	95.2827(16)	95.8959(8)	96.1355(14)	96.314(3)
γ /deg	90.00	93.2657(8)	93.2374(15)	93.044(3)
<i>V</i> /Å ³	983.05(15)	573.328(15)	575.86(8)	583.59(12)
<i>d</i> _{calc} /g cm ^{−3}	1.616	1.594	1.587	1.566
μ /cm ^{−1}	3.47	3.21	3.2	3.16
<i>F</i> (000)	496	288	288	288
2 θ _{max} /deg	58	100	58	58
Number of measured reflections	8779	43756	7024	7084
Number of independent reflections	2585	11721	3055	3085
Number of reflections with $I \geq 2\sigma(I)$	2398	10076	2754	2708
<i>R</i> ₁	0.0493	0.0276	0.0285	0.0319
<i>wR</i> ₂	0.1102	0.0756	0.0842	0.0911
GOF	1.097	1.001	1.079	1.087
Residual electron density ($\rho_{\text{min}}/\rho_{\text{max}}$)/e Å ^{−3}	−0.442/0.443	−0.478/0.597	−0.403/0.354	−0.411/0.336

Table 2. Main crystallographic data and the structure refinement statistics for ammonium compounds 3–6

Parameter	3	4	5	6
Molecular formula	C ₆ H ₈ N ₂ O ₅ S	C ₁₄ H ₂₂ N ₄ O ₁₂ S ₂	C ₁₅ H ₂₂ N ₄ O ₁₁ S ₂	C ₁₀ H ₁₇ N ₃ O ₁₀ S
Molecular weight	220.20	251.24	498.49	371.33
T/K	100	100	100	100
Crystal system	Triclinic	Triclinic	Monoclinic	Triclinic
Space group	<i>P</i> -1	<i>P</i> -1	<i>P</i> 2 ₁ / <i>c</i>	<i>P</i> -1
<i>Z</i>	2	2	4	2
<i>a</i> /Å	6.4936(7)	7.1661(2)	11.6154(11)	5.7212(4)
<i>b</i> /Å	6.7161(7)	7.7807(2)	7.9045(6)	7.8186(6)
<i>c</i> /Å	10.1576(10)	10.4959(4)	23.1326(18)	17.8909(13)
α /deg	86.8752(19)	102.5380(10)	90.00	84.4572(14)
β /deg	82.8042(19)	93.7480(10)	103.344(3)	84.3157(14)
γ /deg	75.5016(19)	114.3530(10)	90.00	70.3722(14)
<i>V</i> /Å ³	425.38(8)	512.48(3)	2066.6(3)	748.37(9)
<i>d</i> _{calc} /g cm ⁻³	1.719	1.628	1.602	1.648
μ /cm ⁻¹	3.8	3.33	3.26	2.78
<i>F</i> (000)	228	262	1040	388
2 θ _{max} /deg	57	99	105	58
Number of measured reflections	4548	59987	298323	8874
Number of independent reflections	2231	10103	24061	3948
Number of reflections with <i>I</i> ≥ 2 σ (<i>I</i>)	1931	8163	17850	3321
<i>R</i> ₁	0.0460	0.0335	0.0339	0.0354
<i>wR</i> ₂	0.1113	0.0946	0.0952	0.0998
GOF	1.053	1.001	1.033	1.045
Residual electron density (ρ _{min} / ρ _{max})e Å ⁻³	−0.711/0.636	−0.431/0.895	−0.473/0.634	−0.388/0.485

multipole refinement are characterized by the following parameters: *R* = 0.0210, *wR* = 0.0214, GOF = 0.917 based on 9975 reflections with *I* > 3 σ (*I*) for 2; *R* = 0.0230, *wR* = 0.0189, GOF = 1.0239 based on 7283 reflections with *I* > 3 σ (*I*) for 4; *R* = 0.0235, *wR* = 0.0212, GOF = 0.9521 based on 16085 reflections with *I* > 3 σ (*I*) for 5.

The potential energy density *v*(**r**) was calculated from the X-ray diffraction data using an approximation in terms of the Thomas–Fermi theory.²⁹ According to this approach, the kinetic energy density (*g*(**r**)) can be calculated by the equation $g(\mathbf{r}) = 3/10(3\pi^2)^{2/3}[\rho(\mathbf{r})]^{5/3} + (1/72)|\nabla\rho(\mathbf{r})|^2/\rho(\mathbf{r}) + 1/6\nabla^2\rho(\mathbf{r})$ combined with the local virial theorem $2g(\mathbf{r}) + v(\mathbf{r}) = 1/4\nabla^2\rho(\mathbf{r})$, which allows calculations of both the potential energy density and the electron energy density *h_e*(**r**). The critical points (3,−1) were found and the corresponding topological characteristics of *p*(**r**), including *h_e*(**r**), *g*(**r**), and *v*(**r**), were calculated using the WINXPRO 1.5.20 program.³⁰ The topological analysis of the theoretically calculated function *p*(**r**) was performed with the use of the AIMAll program.³¹

References

1. R. P. Shibaeva, E. B. Yagubskii, *Chem. Rev.*, 2004, **104**, 5347.
2. G. R. Desiraju, *Angew. Chem., Int. Ed.*, 2007, **46**, 8342.
3. (a) C. G. Vayenas, S. Bebelis, C. Pliangos, S. Brosda, *Electrochemical Activation of Catalysis: Promotion, Electrochemical Promotion and Metal-Support Interactions*, Kluwer Acad./Plenum Publ., New York, 2001, 582 pp.; (b) N. Miura, K. Kanamaru, Y. Shimizu, N. Yamazoe, *Solid State Ionics*, 1990, **40–41**, 452.
4. S. Lengyel, B. E. Conway, in *Comprehensive Treatise of Electrochemistry*, vol. 5, Plenum Press, New York, 1983, p. 365.
5. C. J. T. de Grotthuss, *Ann. Chim. (Paris)*, 1806, **58**, 54.
6. K. D. Kreuer, A. Rabenau, R. Messer, *Appl. Phys. A*, 1983, **32**, 45.
7. K.-D. Kreuer, A. Rabenau, W. Weppner, *Angew. Chem., Int. Ed.*, 1982, **21**, 208.
8. (a) J. B. Goodenough, *Proton Conductor: Solids, Membranes, and Gels—Materials and Devices*, Cambridge University Press, Cambridge, 1992, 581 pp.; (b) K.-D. Kreuer, *Chem. Mater.*, 1996, **8**, 610–641.
9. K. A. Lyssenko, P. Yu. Barzilovich, Yu. V. Nelyubina, E. A. Astaf'ev, M. Yu. Antipin, S. M. Aldoshin, *Izv. Akad. Nauk, Ser. Khim.*, 2009, 31 [*Russ. Chem. Bull., Int. Ed.*, 2009, **58**, 31].
10. Yu. V. Nelyubina, M. Yu. Antipin, K. A. Lyssenko, *Usp. Khim.*, 2010, **79**, 195 [*Russ. Chem. Rev. (Engl. Transl.)*, 2010, **79**, 167].
11. D. Taylor, G. C. Vincent, *J. Chem. Soc.*, 1952, 3218.
12. K. A. Lyssenko, M. Yu. Antipin, *Izv. Akad. Nauk, Ser. Khim.*, 2006, 1 [*Russ. Chem. Bull., Int. Ed.*, 2006, **57**, 1].
13. (a) K. A. Lyssenko, P. Y. Barzilovich, S. M. Aldoshin, M. Yu. Antipin, Y. A. Dobrovolsky, *Mendeleev Commun.*, 2008, **18**, 312; (b) A. Merschenz-Quack, D. Mootz, *Acta Crystallogr., Sect. C: Cryst. Struct. Commun.*, 1990, **46**, 1478; (c) J. Roziere, J. M. Williams, *J. Chem. Phys.*, 1978, **68**, 2896.
14. A. Sillanpää, K. Laasonen, *ChemPhysChem*, 2005, **6**, 1879.

15. Y. V. Nelyubina, S. I. Troyanov, M. Yu. Antipin, K. A. Lyssenko, *J. Phys. Chem. A*, 2009, **113**, 5151.
16. K. A. Lyssenko, D. V. Lyubetsky, M. Yu. Antipin, *Mendeleev Commun.*, 2003, **13**, 60.
17. (a) C. George, J. R. Deschamps, A. P. Purdy, *Acta Crystallogr., Sect. E: Struct. Rep. Online*, 2002, **58**, o1128; (b) N. K. Vyas, T. D. Sakore, A. B. Biswas, *Acta Crystallogr., Sect. B: Struct. Sci.*, 1978, **34**, 3486.
18. *Organicheskie provodniki [Organic Conductors]*, Ed. V. A. Kargin, Nauka, Moscow, 1968, p. 546 (in Russian).
19. B. Giese, *Annu. Rev. Biochem.*, 2002, **71**, 51.
20. (a) G. R. Desiraju, *Crystal Engineering: The Design of Organic Solids*, Elsevier, Amsterdam, 1989, 312 pp.; (b) F. H. Allen, W. D. S. Motherwell, P. R. Raithby, G. P. Shields, R. Taylor, *New. J. Chem.*, 1999, **25**, 24.
21. S. Chandra, N. Singh, *Solid State Ionics*, 1983, **9–10**, 1067.
22. R. F. W. Bader, *Atoms in Molecules. A Quantum Theory*, Oxford University Press, Oxford, 1990, 458 pp.
23. (a) E. Espinosa, E. Molins, C. Lecomte, *Chem. Phys. Lett.*, 1998, **285**, 170; (b) E. Espinosa, I. Alkorta, I. Rozas, J. Elguero, E. Molins, *Chem. Phys. Lett.*, 2001, **336**, 457.
24. (a) L. N. Puntus, K. A. Lyssenko, M. Yu. Antipin, J.-C. G. Bünzli, *Inorg. Chem.*, 2008; **47**, 11095; (b) K. A. Lyssenko, Yu. V. Nelyubina, R. G. Kostyanovsky, M. Yu. Antipin, *ChemPhysChem*, 2006, **7**, 2453; (c) Yu. V. Nelyubina, I. V. Glukhov, M. Yu. Antipin, K. A. Lyssenko, *Chem. Comm.*, 2010, **46**, 3469; (d) Yu. V. Nelyubina, M. Yu. Antipin, I. A. Cherepanov, K. A. Lyssenko, *CrystEngComm*, 2010, **12**, 77.
25. S. Grimme, *J. Comput. Chem.*, 2006, **27**, 1787.
26. B. M. Grafov, E. A. Ukshe, *Elektrokhimicheskie tsepi peregennogo toka [Electric Chains of Alternating Current]*, Nauka, Moscow, 127 pp. (in Russian).
27. G. M. Sheldrick, *SHELXTL-97, Version 5.10*, Bruker AXS, Inc., Madison (WI), USA.
28. A. Volkov, P. Macchi, L. J. Farrugia, C. Gatti, P. Mallinson, T. Richter, T. Koritsanszky, *XD2006 — A Computer Program Package for Multipole Refinement, Topological Analysis of Charge Densities and Evaluation of Intermolecular Energies from Experimental and Theoretical Structure Factors*, 2006.
29. D. A. Kirzhnits, Yu. E. Lozovik, G. V. Shpatakorskaya, *Usp. Fiz. Nauk*, 1975, **117**, 3 [*Physics-Uspekhi, Adv. Phys. Sci., (Engl. Transl.)*, 1975, **18**, 649].
30. (a) A. Stash, V. Tsirelson, *WINXPPO, A Program for Calculation of the Crystal and Molecular Properties Using the Model Electron Density*, 2001; (b) A. Stash, V. G. Tsirelson, *J. Appl. Crystallogr.*, 2002, **35**, 371.
31. T. A. Keith, *AIMAll Version 08.01.25*, 2008, <http://aim.tkgristmill.com>.

Received March 4, 2011